Doppler Frequency Shift in a Refractive Atmosphere

Dipankar Roy*
Boeing Commercial Airplane Company, Seattle, Washington

A general derivation is given for the Doppler-shifted received frequency due to source and receiver motion of uniform velocity in a steady-state, refractive medium with spatial gradients in velocity and temperature. The results from three cases of this generalized equation are especially important. First is the wind tunnel case, in which a stationary noise source is tested; in-flow or out-of-flow measurements at a fixed receiver should show no Doppler frequency shift. Second is the outdoor flyover noise test case, where a source is moving in an atmosphere with wind and temperature gradients. The Doppler frequency effects measured at a stationary microphone are different from those of the zero-wind, isothermal case; actual flyover data support this theoretical result. Third, the generalized Doppler frequency shift equation shows different frequencies of sound received by moving air particles at different heights; these frequencies can be incorporated into an atmospheric absorption model with varying wind and temperature.

Nomenclature

c	= speed of sound ($=$ constant) in an isothermal atmosphere
$c_S, c(z), c_R$	= speed of sound at the source S, at any height z, and at the receiver R, respectively
f_S, f_R	= source and received frequencies
h_S, h_R	= source and receiver heights
k, k_x, k_y	= wavenumber ($= 2\pi$/wavelength λ), its x and y components
M_S, M_R	= source and receiver Mach numbers
t_S, t_R	= sound emission time at source S and sound received time at receiver R
t_{prop}	= noise propagation time from source to receiver
u	= x component of the wind velocity in a uniform wind atmosphere
$u_S, u(z), u_R$	= x component of the wind velocity at the source S, at any height z, and at the receiver R, respectively
u_{S_n}, u_{R_n}	= component along the wavenormal of the wind component u at the source S and at the receiver R
v	= y component of the wind velocity in a uniform wind atmosphere
$v_S, v(z), v_R$	= y component of the wind velocity at the source S, at any height z, and at the receiver R, respectively
v_{S_n}, v_{R_n}	= component along the wavenormal of the wind component v at the source S and at the receiver R
V_{SA}, V_{SG}	= source velocity with respect to the air and the ground, respectively
V_{RA}, V_{RG}	= receiver velocity with respect to the air and the ground, respectively
V_{SG_x}, V_{SG_y}	= x and y components of the source velocity with respect to the ground
x, y, z	= right-handed Cartesian coordinate system where x and y are chosen horizontal, orthogonal directions, and z is vertically up
α_S^*, α_R^*	= angles between the flight direction and the wavenormal at the source and between the flight direction and the wavenormal at the receiver, respectively
β_{SX}	= angle between the source motion direction and the x direction
β_{RX}	= angle between the receiver motion direction and the x direction
λ	= wavelength
$\theta_S^*, \theta^*(z), \theta_R^*$	= angle between the x axis and the projection of the wavenormal of the source-receiver ray at the source S, at any height z, and at the receiver R on the x-y plane, respectively
θ^*	= angle between the x axis and the projection of the wavenormal of the source-receiver ray on the x-y plane in a uniform wind, isothermal atmosphere
$\theta(z)$	= angle between the x axis and the projection of the source-receiver ray direction at any height z on the x-y plane
$\phi_S^*, \phi^*(z), \phi_R^*$	= angle between the vertically upward z axis and the wavenormals of the source-receiver ray at the source S, at any height z, and the receiver R, respectively
ϕ^*	= angle between the vertically upward z axis and the wavenormal of the source-receiver ray in a uniform wind, isothermal atmosphere
$\phi(z)$	= angle between the vertically upward z axis and the source-receiver ray direction at any height z

I. Introduction

FOR a two-dimensional geometry, a previous paper analytically derived the ratio of the received frequency to the source frequency (commonly called the Doppler frequency shift) for the general case of source, receiver, and medium motions with a uniform velocity.[1] This paper is an extension of Ref. 1; here, a three-dimensional geometry is considered where the source and the receiver are in motion with a uniform velocity and the medium is refracting with spatial variations of wind and temperature.

Two selected cases of the generalized formula in Ref. 1 are especially important to airplane noise research: 1) the steady-state wind tunnel case—when the source and receiver are stationary, but the medium is in motion, the result shows no Doppler frequency shift, and 2) the flyover noise case—when the source and the medium are in uniform motion but the receiver is stationary, the result shows a Doppler

frequency shift *different* from the commonly known result for a uniformly moving source, a stationary medium, and a stationary receiver. The flyover noise spectral data presented in Ref. 1 showed trends in agreement with the theoretical results.

Recent results represent the two given cases more accurately than the results from Ref. 1. In freejet wind tunnel noise studies, the microphone is often placed outside the flow; hence, the propagating sound ray is severely refracted at the edge of the flow. For in-flow wind tunnel measurements, the sound ray often encounters spatial inhomogeneities due to boundary layers or other flow-related inhomogeneities and suffers refraction. In outdoor flyover noise measurements, the wind velocities near the airplane are usually much larger than the wind velocities close to the ground; moreover, the temperature also varies spatially between the airplane and the ground. The recent method takes into account these spatial velocity and temperature variations and is therefore more realistic.

Another important application of this result is in the area of atmospheric absorption. Absorption models currently used for outdoor flyover noise analysis assume an idealized, stationary atmosphere and neglect wind. Moving air particles at different heights in the atmosphere see different Doppler-shifted received frequencies; these received frequencies, calculated from the general formula for source and receiver (air particle) motion through a refracting medium, should be used for absorption calculations rather than the received frequency for stationary air.

II.   The Generalized Doppler Frequency Equation

Section A rigorously derives the generalized Doppler frequency equation for a stationary receiver. Section B extends the results from Sec. A by introducing receiver motion.

A.   Stationary Receiver

The received frequency f_R is the time rate of change of the phase ψ and can be written as

$$f_R = \frac{1}{2\pi} \frac{\mathrm{d}\psi}{\mathrm{d}t_R} = \frac{1}{2\pi} \frac{\mathrm{d}\psi}{\mathrm{d}t_S} \cdot \frac{\mathrm{d}t_S}{\mathrm{d}t_R} \tag{1}$$

Here, t_S is the emission time at a source S, t_R is the received time at a receiver R, and they are related to each other by the equation

$$t_R = t_S + t_{\mathrm{prop}} \tag{2}$$

where t_{prop} is the sound propagation time from the source to the receiver. Differentiating both sides of Eq. (2) with respect to the source emission time t_S, we get

$$\frac{\mathrm{d}t_R}{\mathrm{d}t_S} = 1 + \frac{\mathrm{d}t_{\mathrm{prop}}}{\mathrm{d}t_S} \tag{3}$$

Substituting Eq. (3) into Eq. (1) and recognizing that $[1/(2\pi)]\mathrm{d}\psi/\mathrm{d}t_S$ is the source frequency f_S, we get

$$\frac{f_R}{f_S} = 1 \bigg/ \left(1 + \frac{\mathrm{d}t_{\mathrm{prop}}}{\mathrm{d}t_S} \right) \tag{4}$$

Equation (4) shows that if one can determine the rate of change of propagation time with respect to the source emission time $\mathrm{d}t_{\mathrm{prop}}/\mathrm{d}t_S$ for any chosen source-receiver geometry and medium with any wind temperature variation, then one can evaluate the ratio of the received to the source frequency f_R/f_S.
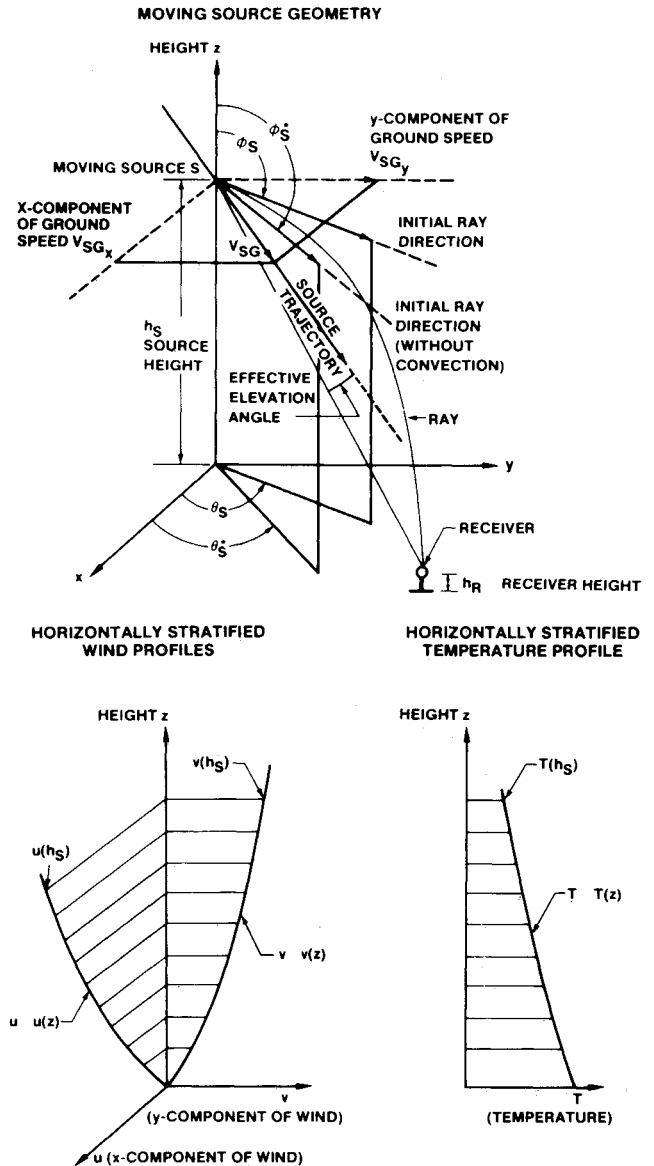

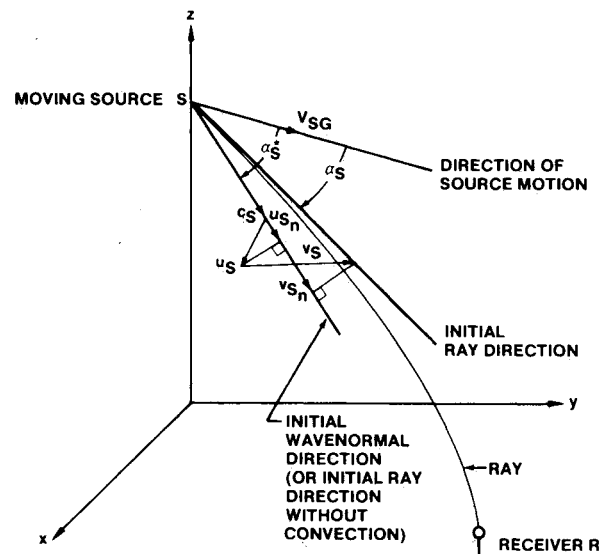Fig. 1a   Sound propagation in three-dimensional stratified atmosphere.

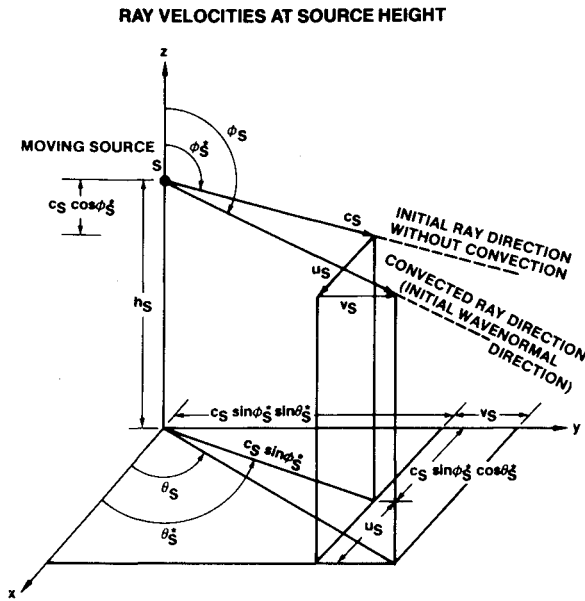Fig. 1b   Angles α_S and α_S^* at the source.
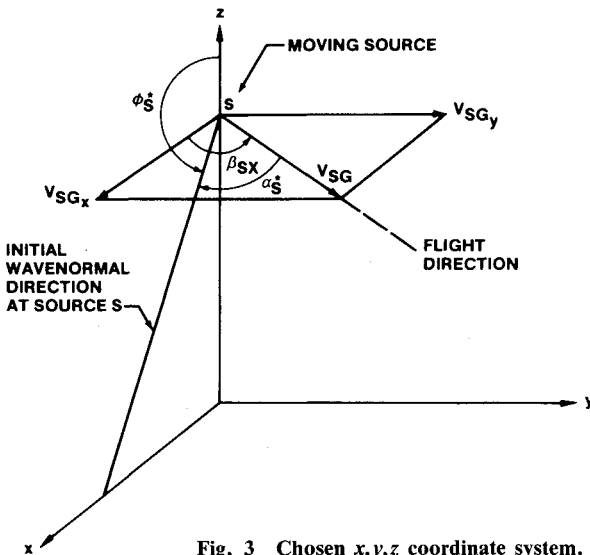
RAY VELOCITIES AT SOURCE HEIGHT

Fig. 2   Velocities at source for the chosen source-receiver ray.

Fig. 3   Chosen x,y,z coordinate system.

Simplified Geometry and Simplified Wind Temperature Profiles

Figure 1a shows a three-dimensional Cartesian coordinate system where x,y are horizontal and z is vertically up. The source moves horizontally at a height h_S, and its velocity with respect to the ground is V_{SG} with V_{SG_x}, V_{SG_y} as its x,y components. The receiver R is at height h_R. The atmosphere is assumed to be horizontally stratified, i.e., its mean wind speeds u,v and temperature T are functions of height z only. The sound emitted at location S at time t_S travels down a ray to receiver R at time t_R.

Ray Equations

Figure 2 shows details of the initial part of the source-receiver ray. The ray velocity with respect to the air is c_S, with polar angle ϕ_S^* and azimuth angle θ_S^*. The wind components u_S, v_S convect this ray so that the initial convected ray velocity with respect to the ground is $c_S + u_S + v_S$, with polar angle ϕ_S and azimuth angle θ_S. It can be shown that although the ray initially points in the direction (ϕ_S, θ_S), the initial wavenormal is in the direction (ϕ_S^*, θ_S^*) with wavespeed $c_S + u_{S_n} + v_{S_n}$, where $u_{S_n} = u_S \cdot c / |c|$ and $V_{S_n} = v_S \cdot c / |c|$ are the wind components in the wavenormal direction. The x,y,z

components of the initial ray velocity are identified in Fig. 2. Generalizing this scenario to any height z, the ray velocity components dx/dt, dy/dt, dz/dt can be given by

$$\frac{dx}{dt} = u(z) + c(z)\,\sin\phi^*(z)\,\cos\theta^*(z) \tag{5a}$$

$$\frac{dy}{dt} = v(z) + c(z)\,\sin\phi^*(z)\,\sin\theta^*(z) \tag{5b}$$

$$\frac{dz}{dt} = c(z)\,\cos\phi^*(z) \tag{5c}$$

where $\phi^*(z)$, $\theta^*(z)$ are the polar and azimuth angles of the wavenormal at any height z, $u(z)$, $v(z)$ are the wind components at height z, and $c(z)$ is the speed of sound, or, more appropriately, the wavespeed with respect to the air.

Expressions for the Rate of Change of Propagation Time t_{prop} with Respect to Source Time t_S

Equation (5c) can be rewritten to give the following expression for the propagation time:

$$t_{\text{prop}} = \int_{h_S}^{h_R} \frac{dz}{c(z)\,\cos\phi^*(z)} \tag{6a}$$

Differentiating both sides of Eq. (6a) with respect to the emission time t_S at the source S gives

$$\frac{dt_{\text{prop}}}{dt_S} = \int_{h_S}^{h_R} \frac{\sin\phi^*(z)}{\cos^2\phi^*(z)}\,\frac{d\phi^*(z)}{dt_S}\,\frac{1}{c(z)}\,dz \tag{6b}$$

Knowing dt_{prop}/dt_S from Eq. (6b), one can solve for the ratio of the received frequency f_R to the source frequency f_S from Eq. (4). The main task now is to obtain expressions for $\sin\phi^*(z)$, $\cos\phi^*(z)$, and $d\phi^*(z)/dt_S$ in Eq. (6b) in terms of the known parameters—initial angles (ϕ_S^*,θ_S^*), wind velocities $u(z)$, $v(z)$, sound speed $c(z)$, and source velocity V_{SG}—so that dt_{prop}/dt_S can be determined.

Relations with Source Velocity Components V_{SG_x}, V_{SG_y}

The ray velocity equations [Eqs. (5)] can be combined to give the following ray-trace equations:

$$x = \int_{h_S}^{h_R} \frac{[u(z) + c(z)\,\sin\phi^*(z)\,\cos\theta^*(z)]\,dz}{c(z)\,\cos\phi^*(z)} \tag{7a}$$

$$y = \int_{h_S}^{h_R} \frac{[v(z) + c(z)\,\sin\phi^*(z)\,\sin\theta^*(z)]\,dz}{c(z)\,\cos\phi^*(z)} \tag{7b}$$

Here, x and y are the horizontal distances from the source S to the receiver R. Differentiating x and y with respect to the emission time t_S gives relationships for the source velocity components V_{SG_x}, V_{SG_y} (see Fig. 1) as follows:

$$\frac{dx}{dt_S} = -V_{SG_x} = \int_{h_S}^{h_R} \left\{ \left[c(z)\,\cos\theta^*(z) + u(z)\,\sin\phi^*(z) \right] \right.$$

$$\times \frac{d\phi^*(z)}{dt_S} - c(z)\,\cos\phi^*(z)\,\sin\phi^*(z)\,\sin\theta^*(z)$$

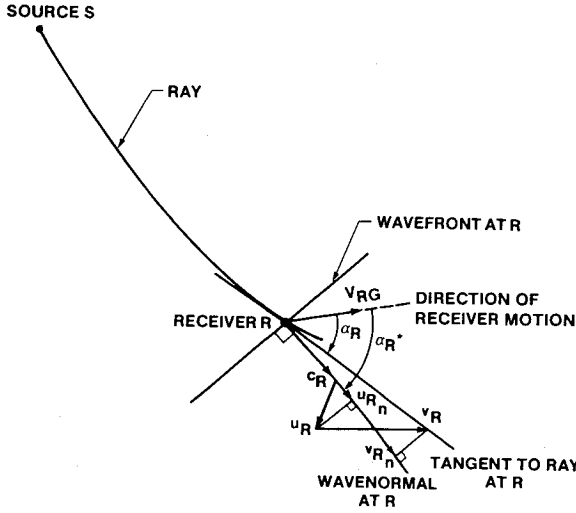$$\left. \times \frac{d\theta^*(z)}{dt_S} \right] dz \right\} \Big/ c(z)\,\cos^2\phi^*(z) \tag{8a}$$

Fig. 4   Moving receiver geometry.

$$\frac{dy}{dt_S} = -V_{SG_y} = \int_{h_S}^{h_R} \left\{ \left[[c(z)\ \sin\theta^*(z) + v(z)\ \sin\phi^*(z)] \right.\right.$$

$$\times \frac{d\phi^*(z)}{dt_S} + c(z)\ \cos\phi^*(z)\ \sin\phi^*(z)\ \cos\theta^*(z)$$

$$\left.\left.\times \frac{d\theta^*(z)}{dt_S}\right] dz \right\} \Big/ c(z)\ \cos^2\phi^*(z) \qquad (8b)$$

The problem is partly solved now—the source velocity V_{SG} has been linked to $\phi^*(z)$, $\theta^*(z)$, $d\phi^*(z)/dt_S$, and $d\theta^*(z)/dt_S$. Expressions for these angles and their rates of change with respect to source time have yet to be determined so that we can calculate dt_{prop}/dt_S; for this, refraction boundary conditions have to be considered.

*Refraction Boundary Conditions
and Horizontal Stratification Simplifications*

Between any two refracting media 1 and 2, where the interface is aligned horizontally, the refraction boundary condition dictates a match of wavenumber components k_x and k_y on both media in any two horizontal directions, i.e.,

$$k_x |_{at\ 1} = k_x |_{at\ 2} \qquad (9a)$$

$$k_y |_{at\ 1} = k_y |_{at\ 2} \qquad (9b)$$

where the wavenumber is defined as $2\pi/\lambda = 2\pi f_R |_{medium}/$ wavespeed. Here, $f_R |_{medium}$ refers to the frequency at any point in the medium with respect to the ground, and wavespeed is also defined with respect to the ground.

If the horizontally stratified atmosphere is now considered as sheets of different media lying one below the other horizontally from the source to the ground, then Eqs. (9) must be satisfied at different sheets along a propagating sound ray. Thus,

$$k_x |_{at\ 1,} = k_x |_{at\ 2} = k_x |_{at\ 3} = ... = k_x |_{at\ any\ height\ z} \qquad (10a)$$
$$\text{i.e., at}$$
$$\text{source}$$

$$k_y |_{at\ 1,} = k_y |_{at\ 2} = k_y |_{at\ 3} = ... = k_y |_{at\ any\ height\ z} \qquad (10b)$$
$$\text{i.e., at}$$
$$\text{source}$$

From Eqs. (10), equating wavenumber components k_x and k_y at the source S and at any height z, we get

$$\frac{2\pi f_R |_{at\ S}\ \sin\phi_S^*\ \cos\theta_S^*}{c_S + u_S\ \sin\phi_S^*\ \cos\theta_S^* + v_S\ \sin\phi_S^*\ \sin\theta_S^*}$$

$$= \frac{2\pi f_R |_{at\ z}\sin\phi^*(z)\ \cos\theta^*(z)}{c(z) + u(z)\ \sin\phi^*(z)\ \cos\theta^*(z) + v(z)\ \sin\phi^*(z)\ \sin\theta^*(z)}$$

$$(11a)$$

$$\frac{2\pi f_R |_{at\ S}\ \sin\phi_S^*\ \sin\theta_S^*}{c_S + u_S\ \sin\phi_S^*\ \cos\theta_S^* + v_S\ \sin\phi_S^*\ \sin\theta_S^*}$$

$$= \frac{2\pi f_R |_{at\ z}\sin\phi^*(z)\ \sin\theta^*(z)}{c(z) + u(z)\ \sin\phi^*(z)\ \cos\theta^*(z) + v(z)\ \sin\phi^*(z)\ \sin\theta^*(z)}$$

$$(11b)$$

Ray Acoustics Approximation

Due to the assumption that the wavenumber is much larger than the scale size of the velocity or temperature discontinuity, it can be shown that refraction in ray acoustics does not change the frequency at stationary observers along a propagating refracted ray.[2] Thus, $f_R |_{at\ S}$ is equal to $f_R |_{at\ z}$ and is canceled from both sides of Eqs. (11). Now Eqs. (11) can be recognized as a three-dimensional "generalized Snell's law" along a ray in the presence of a horizontally moving medium and can be shown to reduce to Kornhauser's[3] and Thompson's[2] results. Note that a wave acoustics solution will show different frequencies suffering different amounts of refraction, i.e., sound from different frequencies will follow different refractive paths between the source and the receiver. From Eqs. (11) we obtain

$$\tan\theta^*(z) = \tan\theta_S^*, \text{ i.e., } \theta^*(z) = \theta_S^* \qquad (12a)$$

$$\sin\phi^*(z) =$$

$$\frac{c(z)\ \sin\phi_S^*}{c_S + [u_S - u(z)]\ \sin\phi_S^*\ \cos\theta_S^* + [v_S - v(z)]\ \sin\phi_S^*\ \sin\theta_S^*}$$

$$(12b)$$

Equations (12) relate $\phi^*(z)$ and $\theta^*(z)$ to the initial angles ϕ_S^* and θ_S^* at the source. These initial angles are assumed either to be known for the ray traced from Eqs. (7) or to be able to be iteratively determined from Eqs. (7) for given source and receiver locations. We still have to determine $d\phi^*(z)/dt_S$ and $d\theta^*(z)/dt_S$ so as to evaluate dt_{prop}/dt_S from Eq. (6b) and hence the received to source frequency ratio f_R/f_S.

Differentiating both sides of Eqs. (12) with respect to the emission time t_S at source S, we get

$$\frac{d\theta^*(z)}{dt_S} = \frac{d\theta_S^*}{dt_S} \qquad (13a)$$

$$\frac{d\phi^*(z)}{dt_S} = \left[c(z) \cdot \left(c_S\ \cos\phi_S^*\ \frac{d\phi_S^*}{dt_S} - \sin\phi_S^*\ \frac{d\theta_S^*}{dt_S} \right.\right.$$

$$\times \{ -[u_S - u(z)]\sin\phi_S^*\ \sin\theta_S^* + [v_S - v(z)]\ \sin\phi_S^*\ \cos\theta_S^* \} \Big) \Big]$$

$$\div (\cos\phi^*(z)\{ c_S + [u_S - u(z)]\ \sin\phi_S^*\ \cos\theta_S^*$$

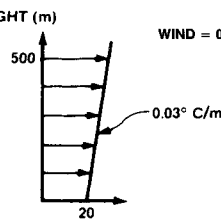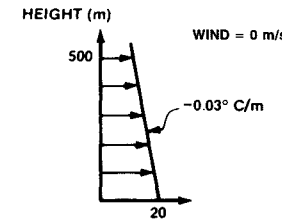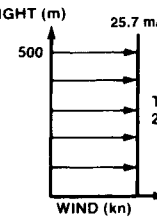$$+ [v_S - v(z)]\ \sin\phi_S^*\ \sin\theta_S^* \}^2) \qquad (13b)$$

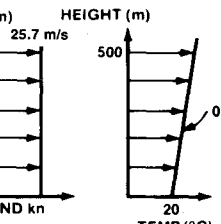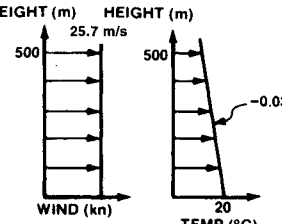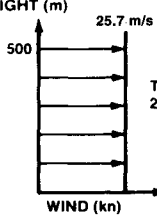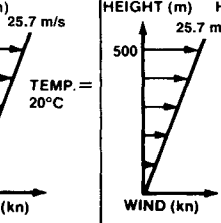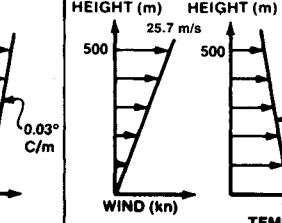| COMPARISONS MADE IN FIGURE NUMBERS	NO WIND, UNIFORM TEMP (IDEAL ATMOSPHERE)*	UNIFORM WIND, UNIFORM TEMPERATURE (CONVECTIVE ATMOSPHERE)**	VARYING WIND, VARYING TEMPERATURE (REFRACTIVE ATMOSPHERE)***	
FIGURES 6a and 6b	TEMP = 20°C WIND = 0 m/s	TEMP. = 20°C WIND = 0 m/s	(Fig. 6a) HEIGHT (m) 500 WIND = 0 m/s 0.03° C/m 20 TEMP (°C)	(Fig. 6b) HEIGHT (m) 500 WIND = 0 m/s −0.03° C/m 20 TEMP (°C)
FIGURES 7a and 7b	TEMP = 20°C WIND = 0 kn	HEIGHT (m) 500 25.7 m/s TEMP. = 20°C WIND (kn)	(Fig. 7a) HEIGHT (m) 500 25.7 m/s WIND kn HEIGHT (m) 500 0.03° C/m 20 TEMP (°C)	(Fig. 7b) HEIGHT (m) 500 25.7 m/s WIND (kn) HEIGHT (m) 500 −0.03° C/m 20 TEMP (°C)
FIGURES 9a, 9b and 9c	TEMP = 20°C WIND = 0 kn	HEIGHT (m) 500 25.7 m/s TEMP. = 20°C WIND (kn)	(FIG. 9a) HEIGHT (m) 500 25.7 m/s TEMP. = 20°C WIND (kn)	(Fig. 9b) HEIGHT (m) 500 25.7 m/s WIND (kn) HEIGHT (m) 500 0.03° C/m 20 TEMP (°C)	(Fig. 9c) HEIGHT (m) 500 25.7 m/s WIND (kn) HEIGHT (m) 500 −0.03° C/m 20 TEMP (°C)

*Eq. (30)   **Eq. (31)   ***Eq. (32)

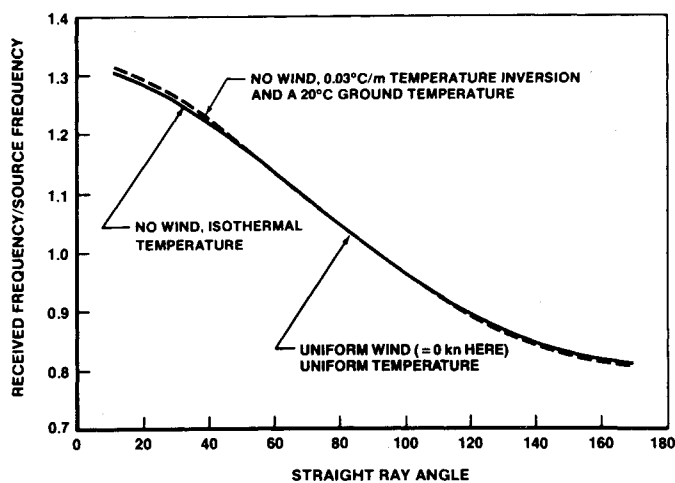**Fig. 5   Selected examples of wind and temperature profiles.**

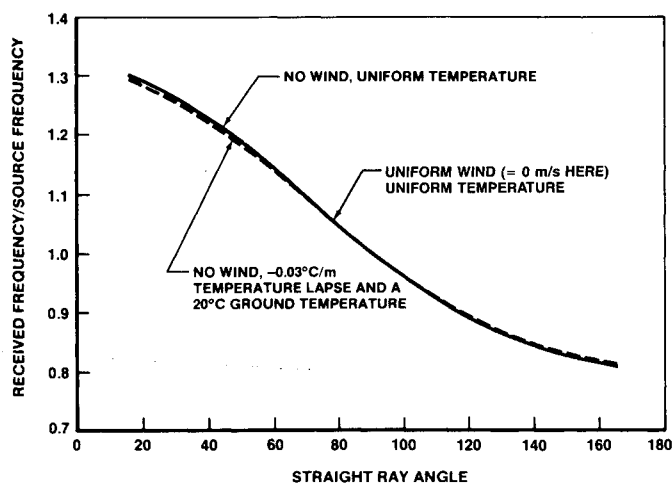**Fig. 6a   Doppler frequencies, temperature inversion.**

Fig. 6b   Doppler frequencies, temperature lapse.

Equations (13) relate $d\phi^*(z)/dt_S$ and $d\theta^*(z)/dt_S$ to $d\phi_S^*/dt_S$ and $d\theta_S^*/dt_S$; the last two quantities are still unknown. However, the relationships with the source velocity—Eqs. (8)—now provide two simultaneous equations with two unknowns, $d\phi_S^*/dt_S$ and $d\theta_S^*/dt_S$, if we substitute the expressions for $\phi^*(z)$, $\theta^*(z)$ from Eqs. (12) and the expressions for $d\phi^*(z)/dt_S$ and $d\theta^*(z)/dt_S$ from Eqs. (13) into Eqs. (8). This gives

$$\begin{bmatrix} A_1 & B_1 \\ A_2 & B_2 \end{bmatrix} \begin{bmatrix} \dfrac{d\phi_S^*}{dt_S} \\ \dfrac{d\theta_S^*}{dt_S} \end{bmatrix} = \begin{bmatrix} C_1 \\ C_2 \end{bmatrix} \tag{14}$$

with solutions

$$\frac{d\phi_S^*}{dt_S} = \frac{\begin{vmatrix} C_1 & B_1 \\ C_2 & B_2 \end{vmatrix}}{\begin{vmatrix} A_1 & B_1 \\ A_2 & B_2 \end{vmatrix}} \tag{15a}$$

$$\frac{d\theta_S^*}{dt_S} = \frac{\begin{vmatrix} A_1 & C_1 \\ A_2 & C_2 \end{vmatrix}}{\begin{vmatrix} A_1 & B_1 \\ A_2 & B_2 \end{vmatrix}} \tag{15b}$$

where

$$A_1 = c_S \cos\phi_S^* \int_{h_S}^{h_R} [c(z) \cos\theta^*(z) + u(z) \sin\phi^*(z)] dz$$

$$\div (\cos^3\phi^*(z)\{c_S + [u_S - u(z)] \sin\phi_S^* \cos\theta_S^*$$

$$+ [v_S - v(z)] \sin\phi_S^* \sin\theta_S^*\}^2) \qquad (16a)$$

$$A_2 = c_S \cos\phi_S^* \int_{h_S}^{h_R} [c(z) \sin\theta^*(z) + v(z) \sin\phi^*(z)] dz$$

$$\div (\cos^3\phi^*(z)\{c_S + [u_S - u(z)] \sin\phi_S^* \cos\theta_S^*$$

$$+ [v_S - v(z)] \sin\phi_S^* \sin\theta_S^*\}^2) \qquad (16b)$$

$$B_1 = \sin^2\phi_S^* \int_{h_S}^{h_R} [c(z) \cos\theta^*(z) + u(z) \sin\phi^*(z)]$$

$$\times \{[u_S - u(z)] \sin\theta_S^* - [v_S - v(z)] \cos\theta_S^*\} dz$$

$$\div \cos^3\phi^*(z)\{c_S + [u_S - u(z)] \sin\phi_S^* \cos\theta_S^*$$

$$+ [v_S - v(z)] \sin\phi_S^* \sin\theta_S^*\}^2 - \int_{h_S}^{h_R} \frac{\sin\phi^*(z) \sin\theta^*(z) dz}{\cos\phi^*(z)}$$

$$(16c)$$

$$B_2 = \sin^2\phi_S^* \int_{h_S}^{h_R} [c(z) \sin\theta^*(z) + v(z) \sin\phi^*(z)]$$

$$\times \{[u_S - u(z)] \sin\theta_S^* - [v_S - v(z)] \cos\theta_S^*\} dz$$

$$\div \cos^3\phi^*(z)\{c_S + [u_S - u(z)] \sin\phi_S^* \cos\theta_S^*$$

$$+ [v_S - v(z)] \sin\phi_S^* \sin\theta_S^*\}^2 + \int_{h_S}^{h_R} \frac{\sin\phi^*(z) \sin\theta^*(z) dz}{\cos\phi^*(z)}$$

$$(16d)$$

$$C_1 = - V_{SG_x} \qquad (16e)$$

$$C_2 = - V_{SG_y} \qquad (16f)$$

The problem can now essentially be solved as follows: $\cos\phi^*(z)$, $\sin\phi^*(z)$, $\cos\theta^*(z)$, $\sin\theta^*(z)$ in Eqs. (16a–16d) can be expressed in terms of known initial angles ϕ_S^*, θ_S^* and known wind and sound speed profiles $u(z)$, $v(z)$, $c(z)$ from Eqs. (12), and thus A_1, A_2, B_1, B_2 in Eqs. (16a–16d) are evaluated. Thus, $d\phi_S^*/dt_S$ and $d\theta_S^*/dt_S$ in Eqs. (15) are determined. From Eq (6b), dt_{prop}/dt_S can then be calculated by first substituting for $\sin\phi^*(z)$ and $\cos\phi^*(z)$ from Eq. (12b) and then substituting for $d\phi^*(z)/dt_S$ from Eq. (13b) where $d\phi_S^*/dt_S$ and $d\theta_S^*/dt_S$ are now known. Since dt_{prop}/dt_S has been determined, f_R/f_S can finally be evaluated from Eq. (4).

Mathematical Simplifications

Although the previously described approach solves the problem computationally, it does not give any physical interpretation of the results. The physics can be seen more easily by carrying out the following mathematical simplifications.

In Fig. 1, the x-y directions were any two arbitrary directions in the horizontal plane. We can therefore arbitrarily choose the x axis to be the horizontal direction such that the initial wavenormal direction and the x and z axes lie on one
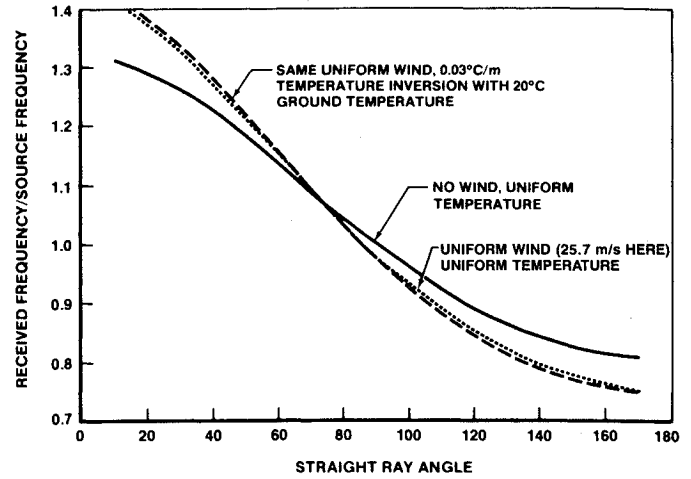

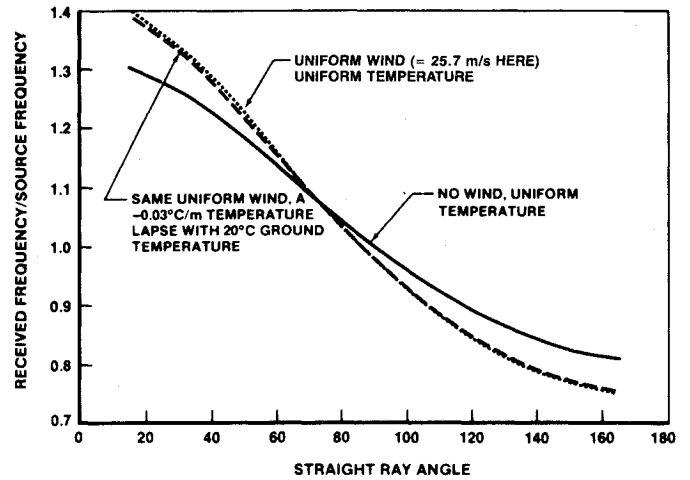Fig. 7a   Doppler frequencies, uniform wind, temperature inversion.

Fig. 7b   Doppler frequencies, uniform wind, temperature lapse.

plane (Fig. 3). Thus, $\theta_S^* = 0$ in this system; this causes considerable simplifications of the previous equations.

Let β_{SX} be the angle between the source motion direction and the x direction (Fig. 3); also, let α_S^* be the angle between the flight direction and the wavenormal direction at the source. Thus,

$$V_{SG_x} = V_{SG} \cos\beta_{SX} \qquad (17a)$$

$$V_{SG_y} = V_{SG} \sin\beta_{SX} \qquad (17b)$$

$$V_{SG} = V_{SG} \cos\beta_{SX}\hat{i} + V_{SG} \sin\beta_{SX}\hat{j} \qquad (17c)$$

Also, unit vector $\hat{m}$ in the wavenormal direction is given by

$$\hat{m} = \sin\phi_S^*\hat{i} + \cos\phi_S^*\hat{k} \qquad (18)$$

Therefore,

$$V_{SG} \cdot \hat{m} = V_{SG} \cos\beta_{SX} \sin\phi_S^* = |V_{SG}| \cdot 1 \cdot \cos\alpha_S^* \qquad (19)$$

i.e., $\cos\alpha_S^* = \cos\beta_{SX} \sin\phi_S^*$. Equations (17) and (19) will subsequently be used in simplifications of the Doppler frequency shift equation.

Since $\theta_S^* = 0$, Eqs. (12) simplify to

$$\theta^*(z) = \theta_S^* = 0 \qquad (20a)$$

$$\sin\phi^*(z) = \frac{c(z) \sin\phi_S^*}{c_S + [u_S - u(z)] \sin\phi_S^*} \qquad (20b)$$

Using Eq. (20a), Eq. (13b) simplifies to

$$\frac{d\phi^*(z)}{dt_S} = c(z)\left(c_S \cos\phi_S^* \cdot \frac{d\phi_S^*}{dt_S} - \sin\phi_S^* \cdot \frac{d\theta_S^*}{dt_S} \cdot \{\sin\phi_S^*\right.$$

$$\left. \cdot [v_S - v(z)]\}\right)\bigg/\left(\cos\phi^*(z)\{c_S + [u_S - u(z)]\sin\phi_S^*\}^2\right)$$

(21)

Using Eqs. (20) and (17), the quantities A_1, A_2, B_1, B_2, C_1, C_2, in Eqs. (16) simplify considerably and are substituted into Eqs. (14) to give expressions for $d\phi_S^*/dt_S$ and $d\theta_S^*/dt_S$. Substituting these expressions into Eq. (21), an expression for $d\phi^*(z)/dt_S$ is obtained in terms of known quantities. Substituting this expression for $d\phi^*(z)/dt_S$ and $\sin\phi^*(z)$ from Eq. (20b) into the expression for dt_{prop}/dt_S in Eq. (6b), one obtains

$$\frac{dt_{prop}}{dt_S} = \frac{-V_{SG}\cos\beta_{SX}\sin\phi_S^*}{c_S + u_S \sin\phi_S^*}$$

(22)

Recognizing that the projections of the wind components at the source on the initial wavenormal direction are given by $u_{S_n} = u_S \sin\phi_S^*$ and $v_{S_n} = 0$, and that $\cos\alpha_S^* = \cos\beta_{SX}\sin\phi_S^*$ from Eq. (19), Eq. (22) can be written as

$$\frac{dt_{prop}}{dt_S} = \frac{-V_{SG}\cos\alpha_S^*}{c_S + u_{S_n} + v_{S_n}}$$

Substituting dt_{prop}/dt_S from the preceding equation into Eq. (4), we get

$$\frac{f_R}{f_S} = 1\bigg/\left(1 - \frac{V_{SG}\cos\alpha_S^*}{c_S + u_{S_n} + v_{S_n}}\right)$$

(23)

Physical Interpretation

For the ray, fixed with respect to the ground, going from the source at S to the receiver R (Fig. 1a), one can explain the Doppler frequency shift by a simple physical explanation. On the ray at the source S, the wavespeed (see Fig. 1b) is given by $(c_S + u_{S_n} + v_{S_n})$ and the wavelength is given by $[(c_S + u_{S_n} + v_{S_n}) - V_{SG}\cos\alpha_S^*]/f_S$. The received frequency on the ray at the source S is the wavespeed divided by the wavelength, i.e.,

$$(c_S + u_{S_n} + v_{S_n})/\{[(c_S + u_{S_n} + v_{S_n}) - V_{SG}\cos\alpha_S^*]/f_S\}$$

$$= f_S/\{1 - [V_{SG}\cos\alpha_S^*/(c_S + u_{S_n} + v_{S_n})]\}$$

Under ray acoustics assumptions, the frequency f_R at the receiver fixed with respect to the ground is equal to the frequency at any other point fixed with respect to the ground on the source-receiver ray SR; hence, f_R is also equal to $f_S/\{1 - [V_{SG}\cos\alpha_S^*/(c_S + u_{S_n} + v_{S_n})]\}$. This corresponds to Eq. (23), derived rigorously. It should again be emphasized that under wave acoustics assumptions, the sound propagation problem to different points of the ray SR is not frequency-independent and will be different from the given ray acoustics solution.

B. Moving Receiver

The wave velocity past the stationary receiver at R (Fig. 4) is $(c_R + u_{R_n} + v_{R_n})$ in the wavenormal direction, where c_R is the wave velocity at R with respect to the air and u_{R_n}, v_{R_n} are components of the wind at R along the wavenormal. Now, consider the receiver in motion (Fig. 4) with velocity V_{RG} with respect to the ground. Only the receiver velocity

component $V_{RG}\cos\alpha_R^*$ changes the wavespeed passing the receiver. The new wavespeed is given by

$$V_w = (c_R + u_{R_n} + v_{R_n}) - V_{RG}\cos\alpha_R^*$$

(24)

The spatial characteristics of the incoming sound waves at R, described by the wavelength λ_R, are unaffected by the receiver motion. Thus, the received frequency at the moving receiver R is given by

$$f_R = \frac{V_w}{\lambda_R} = \frac{c_R + u_{R_n} + v_{R_n}}{\lambda_R} \cdot \left[1 - \frac{V_{RG}\cos\alpha_R^*}{c_R + u_{R_n} + v_{R_n}}\right]$$

The quantity $(c_R + u_{R_n} + v_{R_n})/\lambda_R$ is the received frequency at the stationary receiver, known from Eq. (23). Thus, the preceding equation becomes

$$\frac{f_R}{f_S} = \left(1 - \frac{V_{RG}\cos\alpha_R^*}{c_R + u_{R_n} + v_{R_n}}\right)\bigg/\left(1 - \frac{V_{SG}\cos\alpha_S^*}{c_S + u_{S_n} + v_{S_n}}\right)$$

(25)

Equation (25) is the general equation for the received frequency f_R when both the source and receiver are in uniform motion in a refractive atmosphere.

It is difficult to see from Eq. (25) that there is no Doppler frequency shift when the source and receiver are in parallel motion with the same velocity with respect to the ground. For this purpose, an alternative form of Eq. (25) derived next is useful.

For a horizontally stratified atmosphere, Eqs (11a) and (12a) give

$$\frac{c_R + u_{R_n} + v_{R_n}}{c_S + u_{S_n} + v_{S_n}} = \frac{\sin\phi_R^*}{\sin\phi_S^*}$$

(26)

Also, in the coordinate system shown in Fig. 3, $\cos\alpha_S^* = \cos\beta_{SX}\sin\phi_S^*$ is given by Eq. (19). From Eq. (20a), $\theta_R^* = 0$ and the wavenormal at the receiver R also lies in the x-z plane of the coordinate system in Fig. 3. Thus, for a horizontally moving receiver R, it can be shown that

$$\cos\alpha_R^* = \cos\beta_{RX} \cdot \sin\phi_R^*$$

(27)

where β_{RX} is the angle between the horizontally moving receiver and the x axis.

Using Eqs. (19), (27), and (26) in Eq. (25), one obtains the following alternative form of Eq. (25):

$$\frac{f_R}{f_S} = \left(1 - \frac{V_{RG}\cos\beta_{RX}\sin\phi_S^*}{c_S + u_{S_n} + v_{S_n}}\right)\bigg/\left(1 - \frac{V_{SG}\cos\beta_{SX}\sin\phi_S^*}{c_S + u_{S_n} + v_{S_n}}\right)$$

(28)

It can be seen that if the source and receiver velocities with respect to the ground are equal and parallel, then $V_{SG} = V_{RG}$ and $\beta_{SX} = \beta_{RX}$, and from Eq. (28), $(f_R/f_S) = 1$. Thus, there is no Doppler frequency shift when there is no relative motion between the source and the receiver.

III. Different Combinations of Source, Medium, and Receiver Motions

This section individually discusses selected combinations of source, medium, and receiver motions that are especially important or have been previously used to describe aircraft noise research.

A. Moving Refractive Medium; Stationary Source and Receiver

Here, $V_{SG} = V_{RG} = 0$ and Eq. (25) reduces to

$$f_R/f_S = 1$$

(29)

A good example is the wind tunnel case, where a stationary noise source is tested in a steady-state flow with or without spatial gradients; both in-flow and out-of-flow measurements at stationary microphones show no Doppler frequency shift.

B. Moving Source; Stationary Medium and Receiver

Here, $V_{RG} = 0$, $c_S = c = $ constant and $u_{S_n} = v_{S_n} = 0$. The ray direction SR between the source and the receiver is also the wavenormal direction of the sound travelling from the source S to the receiver R; therefore, $\alpha_S^* = \alpha_S$. Hence, Eq. (25) reduces to

$$\frac{f_R}{f_S} = \frac{1}{1 - M_S \cos\alpha_S} \qquad (30)$$

where $M_S = V_{SA}/c$ is the source Mach number.

The preceding simplified equation has been commonly used in the past to describe the relationships of received frequencies between airplane flyover noise and static engine noise data. Differences between Doppler frequency shifts for this situation and more realistic representations of the atmosphere including wind and temperature effects will be described in Sec. D. Along the source-receiver ray SR, the wavespeed with respect to the ground is c and the wavelength λ_R is $(c - V_{SA} \cos\alpha_S)/f_S$; hence the received frequency $f_R = c/\lambda_R$ is given by Eq. (30).

C. Uniformly Moving Source and Uniformly Moving Medium; Stationary Receiver

In this case, $V_{RG} = 0$, $u_S = u(z) = u = $ constant, $v_S = v(z) = v = $ constant, and $c_S = c(z) = c = $ constant. The source receiver ray SR is straight; however, the wavenormal at any point in the ray SR points in a different direction from the wavenormal. Equation (25) reduces to

$$\frac{f_R}{f_S} = 1 \bigg/ \left(1 - \frac{V_{SG} \cos\alpha_S^*}{c + u_n + v_n}\right) \qquad (31)$$

The preceding equation can represent received frequencies at a stationary microphone during a flyover noise test on a windy day better than that given by Eq. (30); in fact, Eq. (30) is a special case of Eq. (31) when there is no wind. Results for the simplified two-dimensional, uniform wind problem $(v_n = 0)$ in Eq. (31) were derived in Ref. 1; comparisons of Doppler frequency shift results between cases B, C, and D will be described subsequently in Sec. D.

Along the source-receiver ray SR, the wavespeed with respect to the ground is $(c + u_n + v_n)$ and the wavelength λ_R is $[(c + u_n + v_n) - V_{SG} \cos\alpha_S^*]/f_S$; hence, the received frequency $f_R = (c + u_n + v_n)/\lambda_R$ is given by Eq. (31).

D. Uniformly Moving Horizontal Source and Horizontally Stratified Refracting Medium; Stationary Receiver

Here $V_{RG} = 0$ and Eq. (25) reduces to

$$\frac{f_R}{f_S} = 1 \bigg/ \left(1 - \frac{V_{SG} \cos\alpha_S^*}{c_S + u_{S_n} + v_{S_n}}\right) \qquad (32)$$

Equation (32) can be used to calculate the received frequencies at a stationary microphone for flyover noise in the presence of atmospheric wind and temperature with spatial gradients; it is a more realistic and more general representation than flyover noise through an isothermal, uniform wind atmosphere given by Eq. (31).

For the varying wind and temperature atmosphere, the wavespeed at S with respect to the ground along the source-receiver ray SR is $(c_S + u_{S_n} + v_{S_n})$ and wavelength is $[(c_S$

$+ u_{S_n} + v_{S_n}) - V_{SG} \cos\alpha_S^*]/f_S$. In ray acoustics, the received frequency with respect to the ground at any point along the ray SR is the same and equal to

$$\frac{(c_S + u_{S_n} + v_{S_n})}{[(c_S + u_{S_n} + v_{S_n}) - (V_{SG} \cos\alpha_S^*)]/f_S}$$

Hence, the received frequency f_R at the stationary receiver R is given by Eq. (32).

From Eq. (32) it appears that the parameters V_{SG}, α_S^*, c_S, u_{S_n}, and v_{S_n} at only the source are contributing to the Doppler frequency shift. This is a fallacy; it should also be noted that the wind and temperature profiles throughout the region between the source and the receiver determine the source-receiver ray SR and the wavenormal direction at the source S. Thus, the angle α_S^* and the wind components u_{S_n} and v_{S_n} at the source S depend on the entire wind and temperature profiles between the source and the receiver.

For two-dimensional simplifications of Secs. B, C, and D, the computed results for selected wind and temperature profiles (Fig. 5) have been compared. The source Mach number $M_S = V_{SA}/c_S$ in all cases was 0.24 at a height of 500 m; all the windy cases considered were tailwind situations. The chosen wind and temperature profiles (Fig. 5) have linear gradients and perhaps adequately represent the atmospheric variations during outdoor flyover noise testing, between the airplane and a receiver a few feet above the ground. For a receiver very close to the ground, logarithmic wind and temperature profiles for at least the last few feet should be considered. It should also be emphasized that the chosen conditions in Fig. 5 are not representative of other important noise radiation problems, e.g., noise radiation from a high-speed convecting jet-noise eddy through a refracting shear layer.

A no-wind atmosphere and a linear temperature inversion of $0.03°C/m$ (Fig. 6a; also see Fig. 5) or a linear temperature lapse of $-0.03°C/m$ (Fig. 6b) does not change the received to source frequency ratio very much in comparison to the no-wind, isothermal atmosphere situation; the differences become slightly larger at shallow angles. In both Figs. 6a and 6b, the horizontal axis corresponds to the angle between the flight direction and a straight line joining the given source and receiver locations.

Tailwind flyover at a uniform 25.7-m/s-wind, isothermal atmosphere (Fig. 7a) shows received to source frequency ratios quite different in comparison to the no-wind, isothermal situation; this result was already shown in Ref. 1. It was also shown that constant Mach number headwind and tail-
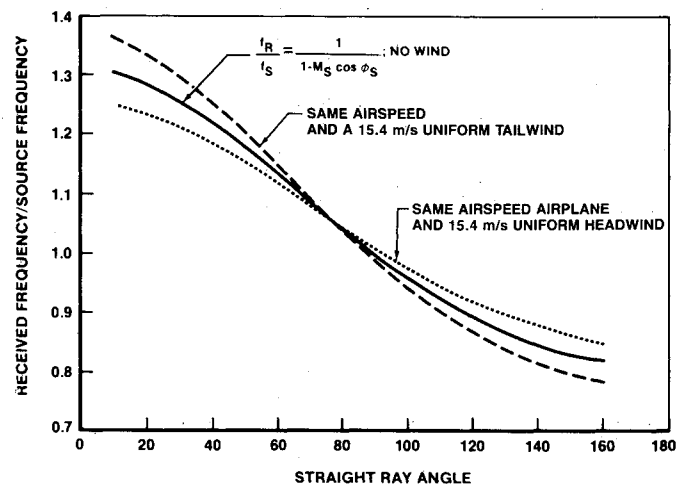

Fig. 8 Headwind and tailwind received to source frequency ratio comparisons for uniform wind.

wind flyovers under a uniform-wind isothermal atmosphere produce Doppler frequency shifts in the opposite sense (Fig. 8, taken from Ref. 1); thus, at a given straight ray angle ϕ, the difference in received to source frequency ratios between tailwind and headwind flyovers under a uniform-wind, isothermal atmosphere is approximately twice that between tailwind flyovers under a uniform-wind, isothermal atmosphere and no-wind, isothermal atmosphere flyovers.
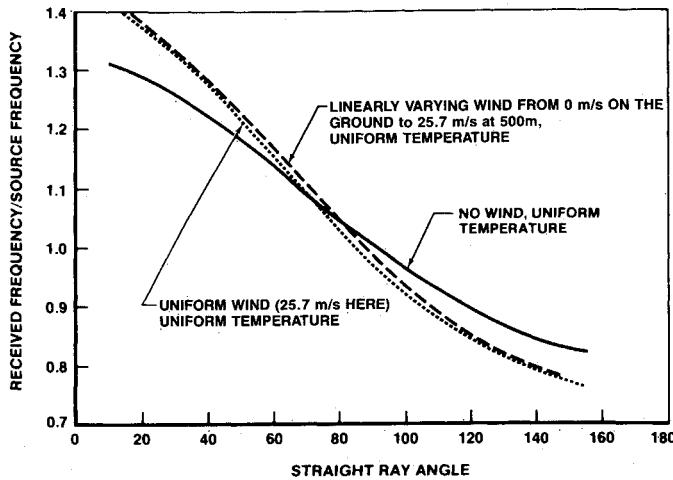

Fig. 9a Doppler frequencies, wind gradient.
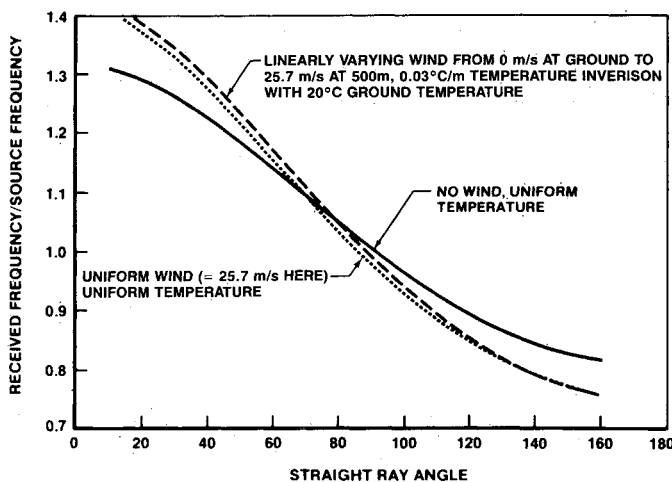
Fig. 9b Doppler frequencies, wind gradient, temperature inversion.
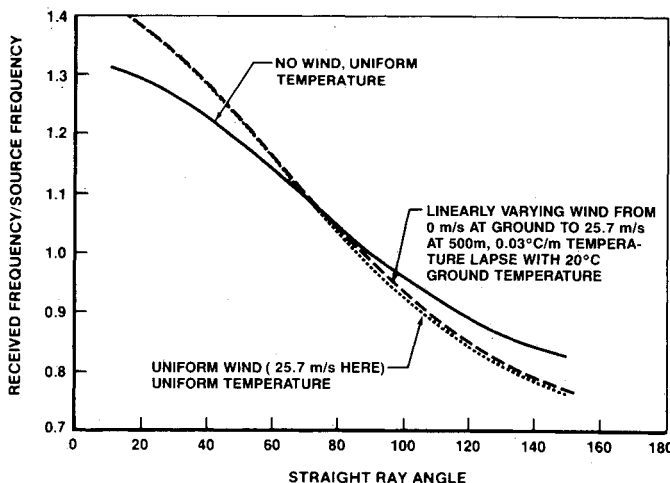
Fig. 9c Doppler frequencies, wind gradient, temperature lapse.

Subsequent computed results pertain to tailwind flyovers only; no further study on headwind-tailwind flyover differences under refractive atmospheres has been made. The superimposition of a linear temperature inversion of 0.03°C/m (Fig. 7a) or a linear temperature lapse of −0.03°C/m (Fig. 7b) on the uniform 2.57 m/s wind does not produce major differences of the received to source frequency ratio in comparison to the results for the uniform 50-kn wind, isothermal atmosphere; these differences become slightly larger at shallow angles.

The received to source frequency ratios for an isothermal atmosphere and linear wind shear from 0 m/s at the ground to 25.7 m/s at the flyover altitude (Fig. 9a) are somewhat different from those for the uniform-wind, isothermal atmosphere results. The superimposition of a linear temperature inversion of 0.03°C/m (Fig. 9b) or a linear temperature lapse of −0.03°C/m (Fig. 9c) on the linear wind shear shows some differences of received to source frequency ratios in comparison to the uniform-wind, isothermal temperature case.

Comparisons at a constant emission angle between back-to-back headwind and tailwind flyover spectral data (see Ref. 1) have shown that tones could lie in adjacent one-third octave bands; it was argued in Ref. 1 that Doppler frequency differences between the two cases obtained from the uniform-wind, isothermal atmosphere model (Fig. 8) show trends similar to the data. In reality, winds close to the ground are generally much smaller than at the airplane flyover altitude. Also, temperature gradients normally exist in the atmosphere—inversions at night and lapses during the day. Thus, the Doppler frequency formulation for the refractive atmosphere would account for the measured data better than that for the uniform-wind, isothermal atmosphere. From the comparisons of these computed results it appears that major differences in the tone frequencies can be accounted for by the uniform-wind, isothermal atmosphere model; somewhat lesser differences can only be accounted for by considering the Doppler frequency effects in a refractive atmosphere.

E. Doppler-Shifted Received Frequencies in Moving Air Particles During Flyovers

For air particles with velocity $[u(z)+v(z)]$ at height z, the generalized Doppler frequency, Eq. (25), reduces to

$$\frac{f_R}{f_S} = \left[1 - \frac{|u(z)+v(z)| \cos\alpha_R^*}{c_R + u_{R_n} + v_{R_n}}\right] \bigg/ \left(1 - \frac{V_{SG} \cos\alpha_S^*}{c_S + u_{S_n} + v_{S_n}}\right) \quad (33)$$

Equation (33) can be used to calculate the Doppler-shifted received frequencies of different air particles along the sound propagation path; these received frequencies could then be incorporated into a proper absorption model through a moving atmosphere with spatially varying winds.

IV. Concluding Remarks

The generalized Doppler-shifted received frequency equation, Eq. (25), shows that only the parameters at the source and at the receiver appear in the final formula. However, the wind and temperature gradients throughout the propagation path are also important because they affect the source-receiver ray and hence the quantities α_R^*, α_S^*, u_{R_n}, u_{S_n}, v_{R_n}, v_{S_n}, c_{R_n}, and c_{S_n} in Eq. (25). Since all the parameters in Eq. (25) are not in terms of the details of the horizontally stratified ray equations assumed for the derivation, it is speculated that the general Doppler frequency result, Eq. (25), is also the ray-acoustics solution for a more general steady-state flow—one that is not horizontally stratified.

It was shown that different specializations of Eq. (25) solved different problems of significant interest to the aircraft noise engineer. In the wind tunnel case, where the source and receiver are stationary and the medium has spatially varying motion, there is no Doppler frequency shift [Eq. (29)]. For received frequencies in the outdoor flyover noise propagation problem, Eq. (32) takes into account the spatial variations of wind and temperature and is an improvement over the uniform-wind, isothermal temperature case [Eq. (31)] and the no-wind, isothermal temperature case [Eq. (30)]. Moving air particles at different heights see propagating sound from an airplane at different frequencies [Eq. (33)]; these frequencies could be incorporated into an absorption model with varying wind and temperature.

References
[1]Roy, D., "Doppler Frequency Effects Due to Source, Medium, and Receiver Motions of Constant Velocity," AIAA Paper 83-0702, April 1983.
[2]Thompson, R. J., "Ray Theory for an Inhomogeneous Moving Medium," *Journal of the Acoustical Society of America*, Vol. 51, No. 5, 1972, pp. 1675–1682.
[3]Kornhauser, E. T., "Ray Theory for Moving Fluids," *Journal of the Acoustic Society of America*, Vol. 25, No. 5, 1953, p. 948.